A continuous model for supply chains with finite buffers

D. Armbruster* S. Göttlich† M. Herty‡

September 21, 2010

Abstract

An aggregate continuum model for production flows and supply chains with finite buffers is proposed and analyzed. The model extends earlier partial differential equations that represent deterministic coarse grained models of stochastic production systems based on mass conservation. The finite size buffers lead to a discontinuous clearing function describing the throughput as a function of the work in progress. Following previous work on stationary distribution of WIP along the production line, the clearing function becomes dependent on the production stage and decays linearly as a function of the distance from the end of the production line. A transient experiment representing the break down of the last machine in the production line and its subsequent repair is analyzed analytically and numerically. Shock waves and rarefaction waves generated by blocking and re-opening of the production line are determined. It is shown that the time to shutdown of the complete flow line is much shorter than the time to recovery from a shutdown. The former evolves on a transportation time scale whereas the latter evolves on a much longer time scale. Comparisons with discrete event simulations of the same experiment are made.

AMS subject classifications: 90B30, 35L65

Keywords: supply chains, production flow networks, conservation laws with discontinuous flux

1 Introduction

Production and supply chain modeling is characterized by different mathematical approaches at different scales: Discrete event simulations are stochastic simulations that reflect the movement of individual parts through individual machines. They are Monte-Carlo type simulations that take considerable simulation time to converge. Continuous models like [1, 3] use partial differential equations to model production flow in an aggregate way, leading to deterministic coarse grained and fast models. Recently those models based on scalar conservation laws have been reformulated in the framework of network models where the dynamics on the arcs is

[1]School of Mathematical and Statistical Sciences, Arizona State University, USA
armbruster@asu.edu
[2]Fachbereich Mathematik, Technische Universität Kaiserslautern, Germany
goettlich@mathematik.uni-kl.de
[3]RWTH Aachen University, Germany
herty@mathc.rwth-aachen.de

governed by a partial differential equation (PDE); see [15, 24, 25]. This approach is inspired by other recent discussions on networks; see, e.g., [6, 10, 13, 15, 26, 27].

In this paper, we want to contribute to the growing body of continuous models by developing a model for supply chains or factories with finite Work In Progress (WIP) buffers. In the original derivation of the continuous model [3] buffers along the production line have unlimited capacity. The mathematical model reflects semiconductor production where the size of a lot typically allows for an unlimited storage capacity along the production line. In reality this is not always true in semiconductor production much less so in production lines of larger items (e.g. cars).

Production lines with finite WIP buffers have been discussed in the review of Dallery and Gershwin [12]. The review considers the stationary behavior of flow lines with finite buffers modeled e.g. as queueing networks discussing a large variety of flow line cases, their associated models and processes. Underlying our continuum model is the assumption that "regular" stochastic events, like the availability of a tool, the availability of an operator, preventive maintenance, machine failures that do not lead to a complete shutdown of large parts of the production lines etc, are captured in the distribution of flow times through a machine. In that case, de Kok [14] showed experimentally and Gershwin [22] used a theoretical approximation to predict a finite steady state production rate for an infinitely long flow line with finite buffers.

We are using a steady state model that is consistent with Dallery and Gershwin's approach [12] to develop a PDE model of a production line with finite buffers that allows us to study transient and other time dependent phenomena. In particular we are interested in the time evolution of a major temporary shutdown of the production line due to a failure and the time evolution of the recovery of the production line once the failure has been repaired. A first qualitative result of our approach is that the time to shutdown of the complete flow line is much shorter than the time to recovery from a shutdown. While this is true even for flow lines that are operated far below capacity, the recovery time for a production line operated close to capacity seems to operate on a diffusive time scale that is much longer than the typical transport time scale. Since continuum models average over the discrete nature of the production steps and production units, statements derived from these PDE models refer to either expectation values over many samples of major shutdowns of production lines or, assuming ergodicity, the behavior of the spread of a shutdown over very large production lines. We show detailed comparison and validation of our model against recent discrete event simulations using the simulator package χ [23, 36].

The fundamental setup is as in [3]. A high volume multi stage production line is considered. Of fundamental interest is the time evolution of the lot-density $\rho(x,t)$ describing WIP at time t at a position x. Here the position $x \in [0,1]$ does not represent physical positions in the factory but the stages or degree of completion in a production process. The factory has a prescribed inflow $\lambda(t)$ at $x = 0$ and an outflow $x = 1$ generated by the production process through the factory. Since mass or WIP is conserved, the system has to satisfy a conservation law of the form

$$\frac{\partial \rho}{\partial t} + \frac{\partial F}{\partial x} = 0. \tag{1}$$

All the important details of the modeling approach are hidden in the exact model for the flux F. Typical models are the adiabatic model $F = v_{eq}(\rho)\rho$ with a suitable equilibrium velocity

$v_{eq}(\rho)$ [3] and the Chapman Enscog model $F = v_{eq}(\rho)\rho + \frac{\partial D\rho}{\partial x}$ [1]. Alternatively, Eq (1) is the first in an infinite hierarchy of conservation laws [2].

Including models of dispatch policies [34] places limits on the flux. However, none of these models have a limit on the size of the density ρ, i.e. they all implicitly assume that the buffers along the production line are infinite and can deal with any amount of WIP. Notice that there is a very similar set of models in traffic modeling [5, 31, 32]. Here finite traffic density has been considered in several macroscopic (continuous) and microscopic (individual driver) models representing the obvious constraint given by the finite length of a car. There is a strong relation between simple follow–the–leader models and macroscopic models, see [4]. In the context of macroscopic models the fundamental paper of Lighthill and Whitham [32] has been the starting point of further investigations. Therein, a model given by (1) has been proposed with F being a continuous and concave function ρ. Already, this suffices to describe the two main characteristics of traffic flow, namely, jams and free flow. The model has been extended to systems [5, 9] and networks [8, 27, 28]. Common to all these traffic models are the following effects: there are two directions of propagation of information and the speed is depending on the local traffic density (and possibly the local velocity). Furthermore, there exists a finite, maximal speed of propagation of information. However, these traffic models are not suitable in the context of production facilities. This is mainly due to the fact that there exists non–local information, a possibly infinite speed of propagation of information due to an external controller and the second process of a buffer unrelated to the local production density.

The rest of this paper is organized in the following way: Section 2 discusses the known phenomenology for the dynamics of production lines with finite buffers based on the work by Gossens [23]. Section 3 develops a mathematical model, section 4 analyzes the model and section 5 develops numerical algorithms and conducts numerical experiments to reproduce the fundamental properties discussed in section 2.

2 Dynamics of production lines with finite WIP buffers

To fix ideas, let us describe the concrete setup of the simulation experiments conducted by Gossens [23]. A linear production line consisting of 100 machines modeled as queues with associated buffers and stochastic (exponentially distributed) exit processes is set up. The first machine is fed by a stochastic arrival process, typically with exponentially distributed inter-arrival times. The storage capacities of each buffer is M parts. All machines are identical with an average processing rate ν.

A typical dynamical experiment of practical interest has the following steps:

1. We assume an empty factory and start producing with an arrival rate $\lambda < \nu$. Given enough time the system will be in steady state characterized through mean WIP buffers along the production line.

2. After the system has equilibrated, we assume that the last machine has a breakdown leading to a complete shutdown at the end of the production line. Machines upstream of the broken last machine continue to produce until the next downstream buffer is full.

At that time the machine stops producing and holds its finished part. After a while the factory shuts down completely since all buffers are full.

3. The last machine is repaired and starts working again with full production rate ν. We assume that the speed of information along the production line is infinitely fast compared to the speed of moving parts. Hence, the whole production line is aware of the fact that the last machine is working again and tries to resume production. The very first machine in the production line is operated in a pull mode: If the machine is available and if the immediate downstream machine has free buffer space, a lot is started. The corresponding arrival rate $\lambda(t)$ will be capped at the original arrival rate λ.

4. Since $\lambda < \nu$, the buffers along the production line drain and will approach their equilibrium values found in step 1.

Based on averages over large ensembles, Gossens [23] made several interesting observations that any useful aggregate model for production lines with finite buffers should reproduce:

- There exists a maximal steady state throughput of the production line given by $\lambda = \lambda_c$. It depends on the maximal buffer level M and it is found that $\lambda_c(M) < \nu$. Figure 1 shows simulated clearing functions $F(\rho)$ for a maximal buffer sizes $M = 5$ and different positions in the supply chain (denoted by 'workstation'). The clearing functions all end significantly below the maximal throughput of the individual machines which is $\nu = 1$.

- The steady–state WIP distribution $\rho_{ss}(x)$ along the production line seems to have three regimes for an inflow close to the capacity of the system, i.e. λ close to λ_c: Two boundary layers at the begin and end of the line and an almost linear decay in x. For small inflow (relative to the capacity of the system) the steady state has no discernible x dependence. Figure 2 shows averages of simulated steady–states for 10 workstations, different buffer sizes and different throughputs, cf. also Figure 3. Figure 2 is consistent with the WIP profile obtained by the convergent approximate algorithm of Gershwin et al. [21] (see Figure 4.11 in [22]).

- After the last machine has shut down, the production line is filled up by a backwards moving wave with a wave speed given by

$$v_{shutdown} = \frac{\lambda}{M - \int_0^1 \rho_{ss}(x)dx}. \quad (2)$$

- The transient dynamics after the last machine has been repaired depends on the influx λ.
  - If $\lambda \approx \lambda_c$ then the factory drains from the end. The system approaches the steady state distribution almost uniformly in space (see Figure 3).
  - If $\lambda < \lambda_c$ then the WIP in the factory approaches the steady state on two different time scales at the two ends of the production lines. WIP is reduced by a wave "eating" into it from upstream and at the same time WIP uniformly drains downstream.

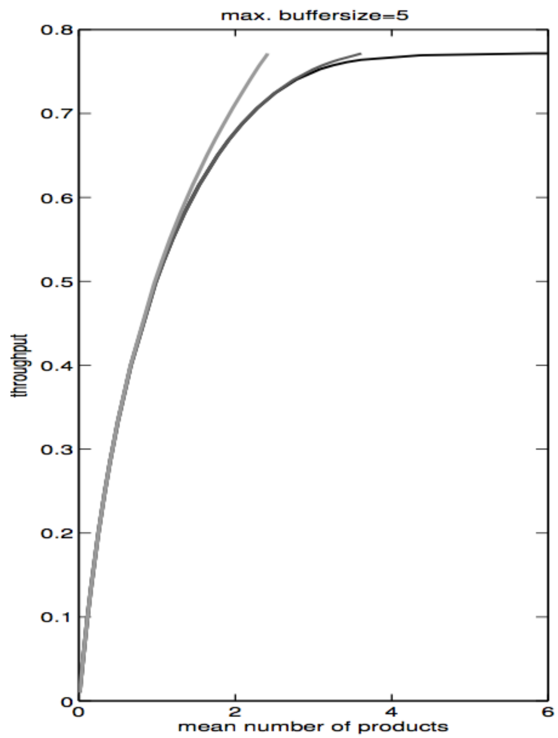

Figure 1: Clearing functions generated by discrete event simulations of a model with 10 workstations and maximal buffer size of $M = 5$. From left to right the curves represent workstation $10, 5$ and 1 (Figure 5.4 [23]).

3 The model

We derive a model under the assumption that the amount of parts and the number of steps justify a continuous model. The previously introduced continuum model [1] was based on mass conservation and spatially homogeneous clearing functions or equilibrium velocity models (see eq. (1)). As a result, equilibria are independent of the space variable x .

Assuming an $M/M/1$ queue, elementary queueing theory gives us the mean cycle-time τ through the queue as $\tau = \frac{1}{\nu - \lambda}$. Calling ρ the average number of parts in the queuing system, Little's law becomes $\tau\lambda = \rho$. Eliminating τ and solving for λ we get the clearing function

$$\lambda = \frac{\nu\rho}{1+\rho}. \tag{3}$$

If we identify λ with the steady state flux F and ρ with the amount of WIP in the production process, Eq. 3 is the state equation for our PDE model and the $M/M/1$ clearing function used e.g. in [1].

We want to introduce a phenomenological model that captures the influence of the finite buffers, in particular the non-homogeneous steady states and the discontinuous fluxes observed in the experiments discussed in section 2 by extension of the homogeneous model. In particular Little's Law [33] still holds true, i.e. mass is conserved and hence the fundamental structure

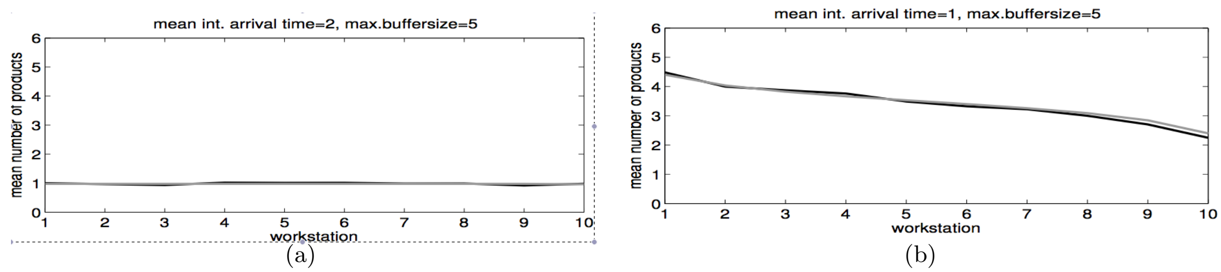

Figure 2: Steady–states generated by a $\chi-$simulation of a model with 10 workstations. a) for $\lambda << \nu$, b) for $\lambda \approx \lambda_c$. Figure 4.2 [23])

of the model is still a conservation law of the form

$$\rho_t + F_x = 0,\ x \in [0,1], t \geq 0, \tag{4}$$

for the density $\rho(x,t)$ with maximum density $\rho_{\max} = M$.

Our fundamental observation is that the probability to move through the jth machine and arrive at the next buffer $j+1$ depends on two stochastic processes now: the machine process that has exponentially distributed departure times with a mean of ν and the process describing the buffer levels and in particular the probabilities that the buffer level become M and hence the $j+1$ buffer is full and therefore the jth machine has to be idle. Barring a first principle theory for the stochastic buffer process, we assume that the probability that the next buffer is full linearly increases with the distance from the end of the production line. In particular, that probability is zero for the last machine since it feeds the outside and we assume an infinite outside inventory. Our fundamental assumption therefore is that the processing rate of the machine becomes inhomogeneous of the form

$$\tilde{\nu} = c(x)\nu.$$

We make three assumptions for $c(x)$;

- $c(1) = 1$.
- $c(x)$ linearly increases with the steady state influx λ, reflecting the fact that the inhomogeneity is small for small fluxes.
- $c(x)$ linearly decreases as a function of x.

A processing rate $\tilde{\nu}$ that is consistent with all three assumptions is

$$\tilde{\nu} = c(x)\nu = \lambda k(x-1) + \nu,$$

with $k > 0$ the decay rate of the processing rate along x. k is a monotone increasing function of the buffer limit M. Following the procedure to get to the clearing function (Equation 3) we find the inhomogeneous, discontinuous clearing function

$$F(\rho, x) := \begin{cases} \frac{\nu\rho}{1+\rho+k\rho(1-x)} & \text{for } \rho < M \\ 0 & \text{for } \rho \geq M. \end{cases} \tag{5}$$

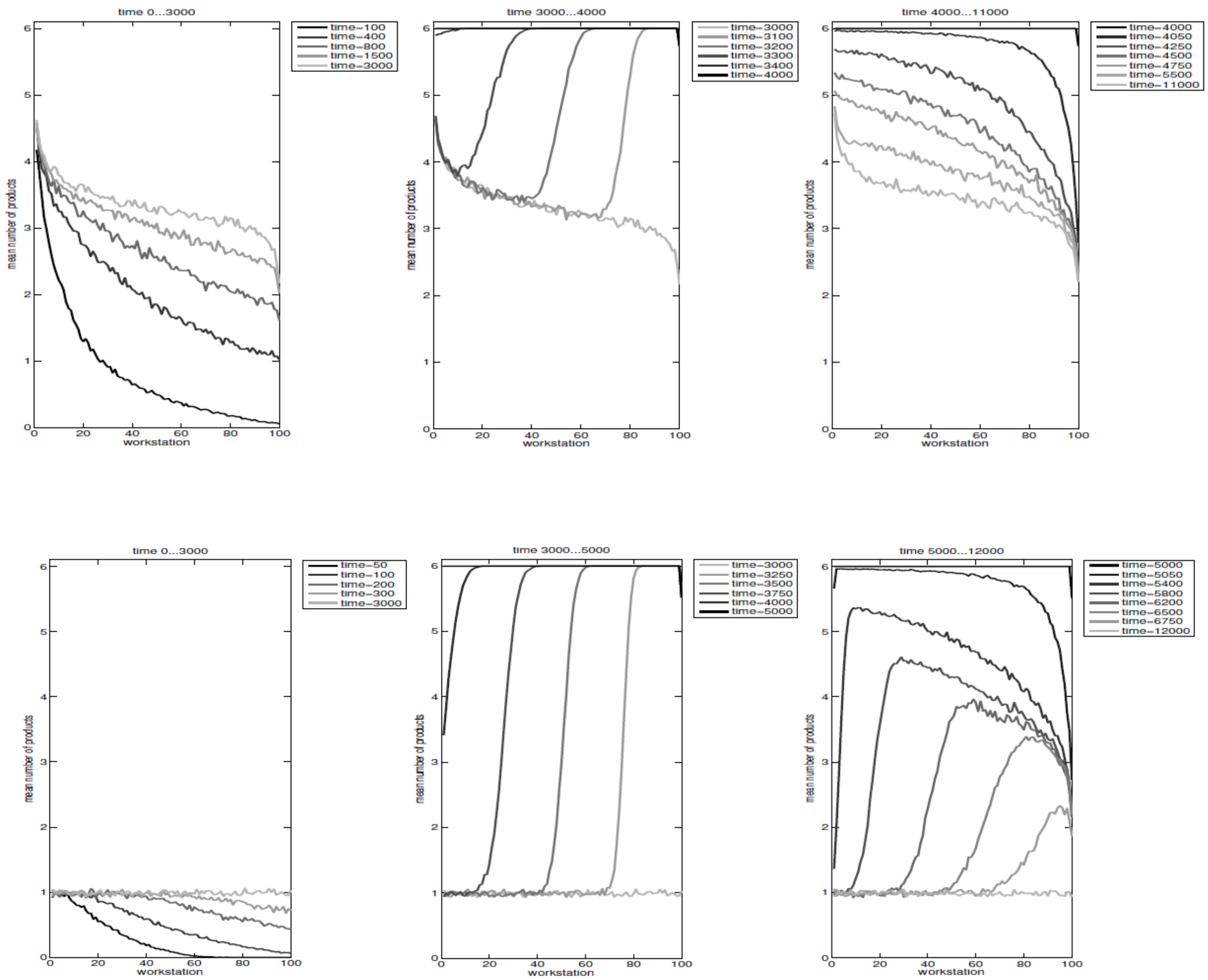

Figure 3: Computational results from a $\chi-$simulation for two different settings: $\lambda \approx \lambda_c$ (first row) and $\lambda << \nu$ (second row), cf. Figure 3.6 in [23]. We observe the following phenomena from left to the right: ramp up and steady state - breakdown of the last machine and backward-moving waves - draining of excess WIP after the final machine has been repaired and production has been restarted. The figure shows snapshots of movies as sequential WIP profiles.

Equation (4) and Equation (5) have to be supplemented by suitable boundary conditions. We impose them in the sense of [7]. This will be discussed below in more detail. Furthermore, a density distribution $\rho(0, x) = \rho_0(x)$ at initial time $t = 0$ has to be prescribed. Figure 4 shows three graphs of the clearing function (5) at three different positions along the production line (cf. see Figure 1).

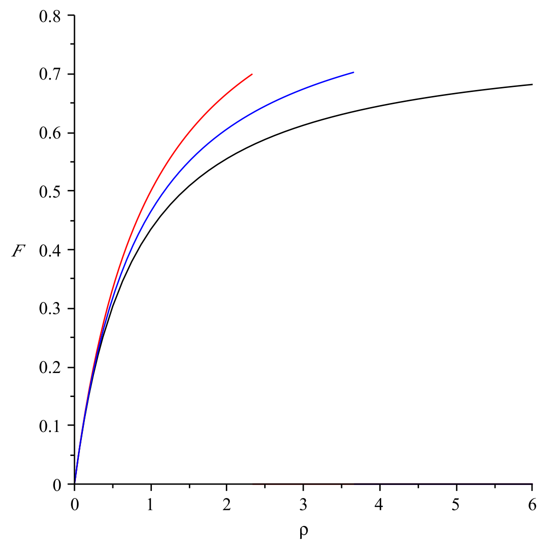

Figure 4: Flux functions (5) at positions $x = 0, 0.5, 1$ in the supply chain.

4 Model features

4.1 Boundary conditions

For production flow lines or supply chains typically an inflow $\lambda(t)$ at $x = 0$ and/or an outflow $\mu(t)$ at $x = 1$ is given. Due to the lack of monotonicity of the flux function F we might not be able to fulfill the conditions $\lambda(t) = F(\rho(0,t), 0)$, $\mu(t) = F(\rho(1,t), 1)$ at all times t. Hence, we prescribe the inflow and outflow conditions in the weak sense of Bardos et. al. [7]. We denote by $\rho(0+,t) = \lim_{x\to 0, x\geq 0} \rho(x,t)$ and similarly by $\rho(1-,t) = \lim_{x\to 1, x\leq 1} \rho(x,t)$. Let $\rho_\lambda \in [0, M)$ be the unique density such that

$$F(\rho_\lambda, 0) = \lambda \tag{6}$$

and $\rho_\mu \in (0, M]$ such that

$$F(\rho_\mu, 1) = \mu. \tag{7}$$

Then, for given densities ρ_λ and ρ_μ the following boundary conditions hold true at all times

t [7].

$$\max_{k \in I(\rho_\lambda(t), \rho(0+,t))} \Big\{ sgn(\rho(0,+,t) - \rho_\lambda(t))(F(\rho(0,t),0) - F(k,0)) \Big\} = 0, \tag{8}$$

$$\min_{k \in I(\rho_\mu(t), \rho(1-,t))} \Big\{ sgn(\rho(1-,t) - \rho_\mu(t))(F(\rho(1-,t),1) - F(k,1)) \Big\} = 0. \tag{9}$$

Consider the inflow boundary at $x = 0$. If $\rho(0+, t) = M$, then (8) holds true independent of the choice of ρ_λ. This is consistent with the observation: if the supply chain is blocked, no more parts can enter. If on the other hand $\rho(0+, t) < M$, then condition (8) implies that $\rho(0+, t) = \rho_\lambda$ or

$$F(\rho(0+, t), 0) = \lambda.$$

Similarly, at the outflow boundary $x = 1$ we obtain that $\rho(1-, t) < M$ implies that (9) holds true for any prescribed outgoing density ρ_μ. On the other hand, if $\rho(1-, t) = M$, then necessarily $\rho_\mu = M$ and vice versa.

The formulation 8 and 9 ensures that the boundary conditions are compatible with the weak formulation of the conservation law [7]. It is well–known that in case of a differentiable flux function F the problem (1) and (8),(9) is a well–posed problem.

4.2 Steady states

The boundary conditions also allow to compute the steady states, i.e. the WIP profiles in equilibrium. In steady state we have

$$\frac{\partial F(\rho(x), x)}{\partial x} = 0 \tag{10}$$

and hence

$$F(\rho(x), x) = \tilde{c}. \tag{11}$$

The constant $\tilde{c}$ is given by the boundary conditions (8) and (9) at $x = 0$ and $x = 1$, respectively. $\rho(x) = 0$ is a steady state if and only if $\rho_\lambda = 0$ and this state satisfies the boundary condition at $x = 1$ for any boundary density ρ_μ. If at some point x_0 we have $\rho(x_0) = M$, then the constant $\tilde{c}$ is necessarily equal to zero. Hence, (11) implies that at any other point x we either have $\rho(x) = 0$ or $\rho(x) = M$. Hence, the only continuous steady state in this case is $\rho(x) = M$. satisfying the boundary condition at $x = 0$ for any incoming density ρ_λ implying $\rho_\mu = M$.

If $0 < \rho < M$ for all x., equation (9) is satisfied for all ρ_μ and we have $\rho(x = 0) = \rho_\lambda$ which defines $\tilde{c}$ as $\tilde{c} := \frac{\nu \rho_\lambda}{1 + \rho_\lambda(1+k)}$. Let $F(\rho, x) := \frac{\nu \rho}{1 + \rho + k\rho(1-x)}$, then F is strictly monotone in ρ for all x. Therefore,

$$\rho(x) = F^{-1}(\tilde{c}, x) = -\frac{\tilde{c}}{\tilde{c}(1 + k - kx) - \nu}. \tag{12}$$

is the well–defined steady state. An easy computation shows that

$$\partial_x \rho(x) < 0 \tag{13}$$

for any $\nu > 0$ and k. This coincides with the observations in the discrete event simulations (Figure 2). In Figure 5 we present steady states for the flux functions of Figure 4 and different values of the influx λ.

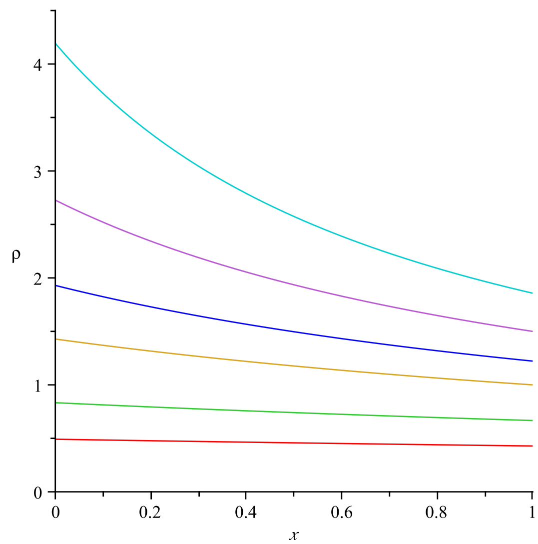

Figure 5: Steady states (Eq. 12) for different values of the influx λ

Remark 4.1.

- *While the decay in of the steady state profile in x is obviously not linear, comparing Figure 5 and 2 shows a good match for all but the largest inflows.*
- *The steady–state calculations hold true for any flux function that is strictly monotone in ρ for $\rho < M$ and is continued by $F = 0$ for $\rho \geq M$.*

We summarize our findings in the following proposition.

Proposition 4.1. *Consider the conservation law (4) with flux function (5) and boundary conditions of the type (8) and (9). Assume inflow λ and outflow μ are such that ρ_λ (6) and ρ_μ (7) are well-defined. Then, there exist three continuous steady states $x \to \rho(x)$ of the conservation law: i) If $\mu = 0$ and $\lambda = 0$, then $\rho = 0$; ii) if $\mu = 0$ and $\lambda > 0$, then $\rho = M$; iii) in all other cases the steady state is given by equation (12).*

4.3 Riemann Problem

Focussing on the discontinuity in the flux function and neglecting the dependence of the flux on x. we can reformulate the conservation law as

$$\rho_t + \partial_x H(M - \rho) f(\rho) = 0, \tag{14}$$

for some strictly monotone, smooth function f and the Heaviside function $H(\cdot)$. To understand dynamical behavior of equation (14) we study the associated Riemann problem. The Riemann problem is a Cauchy problem with piecewise constant initial data ρ_l and ρ_r as

$$\rho(x,0) = \begin{pmatrix} \rho_l & x<0 \\ \rho_r & x>0 \end{pmatrix}. \tag{15}$$

Related conservation laws with discontinuous fluxes have been discussed in [17, 19, 20] and the references therein. In particular, in [18] an analysis of a Riemann problem for nonlinear scalar equation with discontinuous flux function has been investigated. In the case $\rho_l < \rho_r$ there is a notion of solutions even for a discontinuous flux function of the type (14) and the solution can be constructed by considering the lower convex envelope of $H(M-\rho)f(\rho)$. The construction is then precisely as in the continuous case, (see [11]). In [18] properties of this solution and approximations to the flux function have been studied and a notion of entropy solutions has been developed. If we apply these results to the case $H(M-\rho)f(\rho)$, we can characterize the solutions as follows:

- For $0 \leq \rho_l < \rho_r < M$ the solution to the Riemann problem is a classical shock wave with speed $s = \frac{f(\rho_r)-f(\rho_l)}{\rho_r-\rho_l}$
- For $0 \leq \rho_r < \rho_l < M$ the solution to the Riemann problem is a classical rarefaction wave traveling with speed $\tilde{s} = f'(\rho)$.
- For $0 \leq \rho_l < \rho_r = M$ the solution to the Riemann problem is a shock wave traveling with speed $s = \frac{f(\rho_l)}{\rho_l - M}$. Indeed, the lower convex envelope of $\rho v = H(M-\rho)f(\rho)$ can be found by considering the line in the $(\rho, \rho v)-$plane connecting $(\rho_l, f(\rho_l))$ to $(M, 0)$. The slope of this line is the wave speed.

Unfortunately, the case $M = \rho_l > \rho_r$ is not covered in [18]. The reason is as follows: consider a smooth approximation f_ϵ of $H(M-\rho)f(\rho)$ by connecting the point $f(M-\epsilon)$ to 0 by a line of slope $\frac{1}{\epsilon}$. In the case $M = \rho_l > \rho_r$ and for the flux function f_ϵ, the solution consists of a rarefaction wave fan with speed $\tilde{s} = f'(\rho)$. Hence, for $M - \epsilon < \rho < M$, the rarefaction moves with speed $-\mathcal{O}(\frac{1}{\epsilon})$. It is then followed by a rarefaction wave connecting $M - \epsilon$ to ρ_r. The latter is a wave of positive speed. Decreasing ϵ, implies faster and faster backwards moving waves connecting $\rho_l = M$ to $M - \epsilon$. This is an **unphysical process**; however, it is justified in the context of production lines due to step 3 in Section 2. Hence,

- For $0 \leq \rho_r < \rho_l = M$ the solution to the Riemann problem is a wave with speed negative infinity connecting the points $(M, 0)$ and $(M, f(M))$ in the phase space $\rho - \rho v$. This wave is followed by a classical rarefaction wave of positive speed connecting on the left $(M, f(M))$ to $(\rho_r, f(\rho_r))$.

Note that in the case $\rho_l < \rho_r$, the lower convex envelope of f_ϵ coincides with the one of f and we obtain precisely the previously stated solutions also as solutions to the smoothed version of the conservation law (see [18]). Therefore, the smoothing does not affect the construction for $\rho_l < \rho_r$.

Using the previous notion of a solution we observe that this model recovers step 3 and explains step 2 of Section 2. The speed of the backwards moving information in this case is given by $s = \frac{f(\rho_l)}{\rho_l - M}$.

Returning now to the full model (3) and (5) we observe that this model is a conservation with a spatially dependent flux. However, for $\rho < M$ we have that $x \to F(\rho, x)$ is monotone increasing in x and therefore no $\delta-$concentrations can appear in this model. This is consistent with the steps 1–4 in section 2.

5 Numerical experiments

5.1 Analytical solutions

Before turning to the numerical results for the inhomogeneous flux function we present some analytical solutions in the homogeneous situation illuminating the phenomena observed by Gossens [23]. For this discussion we assume a spatially homogeneous flux function and we linearly smooth out the discontinuity of the flux function over a length of ϵ (see Figure 6).

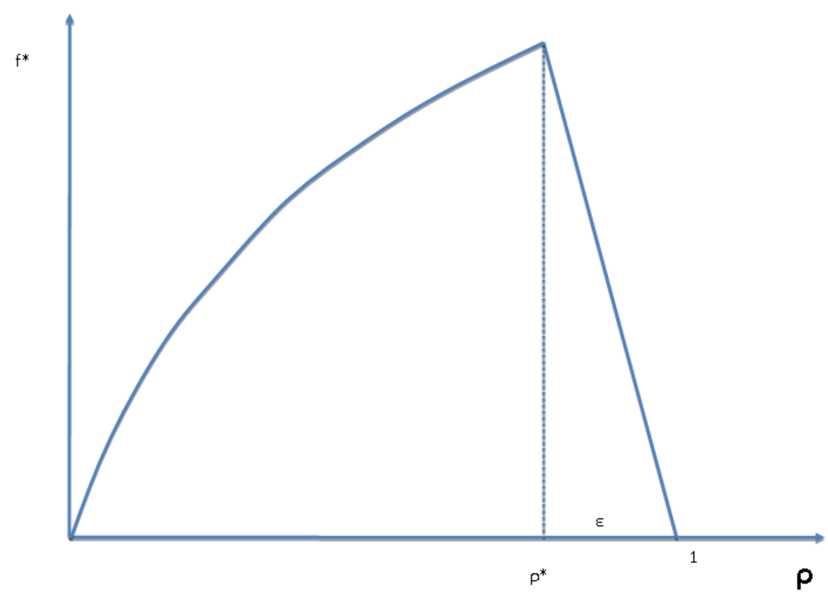

Figure 6: Prototype of the smoothed flux function with a linear connection of the point of maximal flux (ρ^*, f^*) to the point of maximal density $(1, 0)$ on a length of ϵ.

To avoid explicitly treating the boundary conditions we enlarge the spatial domain and consider an initial value problem with three densities $(\rho_\lambda, \rho_0, \rho_\mu)$ in the areas $x \leq 0, 0 < x < 1$ and $x \geq 1$, respectively. The original production line is located at $x \in [0, 1]$. ρ_λ is the inflow density and ρ_μ the outflow density. The dynamics is given by the conservation law $\partial_t \rho + \partial_x F = 0,\ x \in [0, 1]$ with F as in Figure 6 having a maximal flux of f^* for a density ρ^*. We consider now two different situations resembling the observations by Gossens.

At first, we consider the case where the initially empty supply chain fills and is blocked.

This corresponds to choosing initial data $\rho_\lambda < \rho^*, \rho_0 = 0$ and $\rho_\mu = 1$. The solution to the arising Riemann problems is depicted in Figure 7. We observe a stationary shock wave at the boundary $x = 1$ and a rarefaction wave emerging at $x = 0$. Once the rarefaction interacts with the shock the information on the full buffers is transported backwards by a shock–wave.

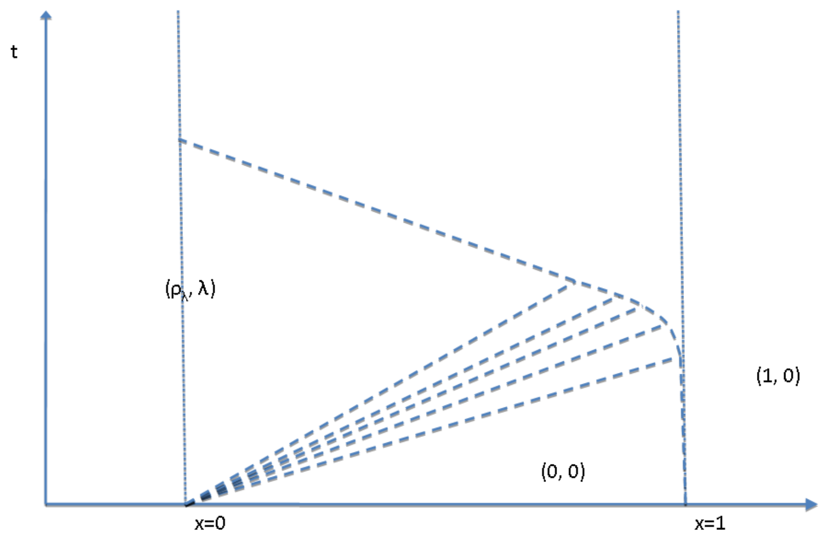

Figure 7: Solution to the initial filling and blocking of the supply chain. The solution in the $x-t-$plane is shown. The solution outside the dotted areas is constant with density and flux as indicated.

Second, we consider the case of a blocked supply chain which reopens at time $t = 0$ for some inflow ρ_λ. The initial data is therefore $\rho_\lambda < \rho^*, \rho_0 = 1$ and $\rho_\mu < \rho^*$. The analytical solution is shown in Figure 8. We observe a fast wave of speed $1/\epsilon$ moving through the supply chain and transporting the maximal density ρ^*. Eventually, this wave interacts with the boundary condition ρ_λ giving rise to a new shock wave moving forward. The rarefaction wave of positive speed emerging at $x = 1$ does not show up within the x-interval of the production line. Note that in the case $\rho_\lambda = \rho^*$ there is no wave entering from $x = 0$ into the production line. This corresponds to the case $\lambda \approx \lambda_c$ or $\rho_\lambda = \rho^*$ in the discrete event simulations (not shown in the figure).

5.2 Numerical solutions

We present a suitable discretization of (4) and (5) to emphasize the applicability of the proposed PDE model to capture the steps 1–4 in Section 2. The numerical approximation of the flux (5) requires care due to the discontinuity in the flux function. We use a Lax-Friedrich scheme for a smoothed out version. In all experiments, we stick to the unit-interval $[0, 1]$, a time horizon of $T = 6$ and a maximal density of $M = 1$. The two parameters in (5) are fixed to $k = 0.7$ and $\nu = 2$. Not surprisingly, the analytical steady state solution according to (12) are reproduced. The reproduce steps 1–4 of the time dependent experiment simulated

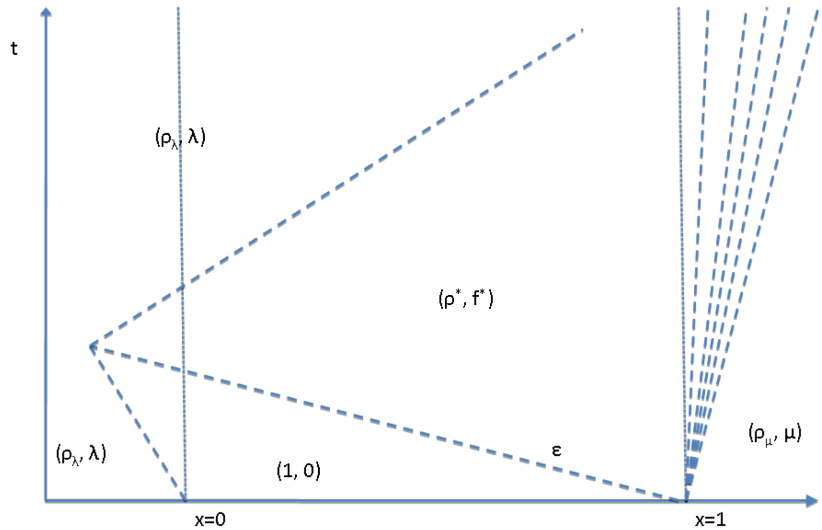

Figure 8: Solution to the reopening of an initially blocked production line. The solution in the $x-t-$plane is shown. The solution outside the dotted areas is constant with density and flux as indicated.

by Gossens we need correct boundary values. We distinguish between three cases:

(i) We choose the inflow density ρ_λ at the left boundary and assume no boundary condition at $x = 1$. This is reasonable due to the monotone increasing flux-function for $\rho < M$.

(ii) When the last machine is blocked, we set boundary conditions $\rho = M$ at the right end. As soon as the backward-going shock arrives at $x = 0$, the condition ρ_λ will be removed.

(iii) Once the last machine has been repaired we set $\rho|_{x=1} = \rho_\mu$.

(iv) After a while, the condition at $x = 1$ is cleared and we again prescribe $\rho|_{x=0} = \rho_\lambda$.

Furthermore, we we need a stable discretization to treat the discontinuity in (5). One possibility to get a numerically tractable scheme is to smooth out the discontinuity. This can be done by a linear approximation at any density ρ^* close to M, see Figure 9. Apparently, the steeper the slope, the better the approximation to the original flux function.
The smoothed out flux function can be solved using a first-order Lax-Friedrichs scheme. Therefore, we introduce a uniform space-time grid satisfying the CFL condition

$$\Delta t \leq \frac{\Delta x}{|f'(\rho)|}$$

with 500 space discretization points. Note that the disadvantage of this smoothing is that extremely steep slopes will lead to small step sizes Δt and thus to high computational costs. However, the qualitative behavior of the solution is independent of the choice of ρ^*. In

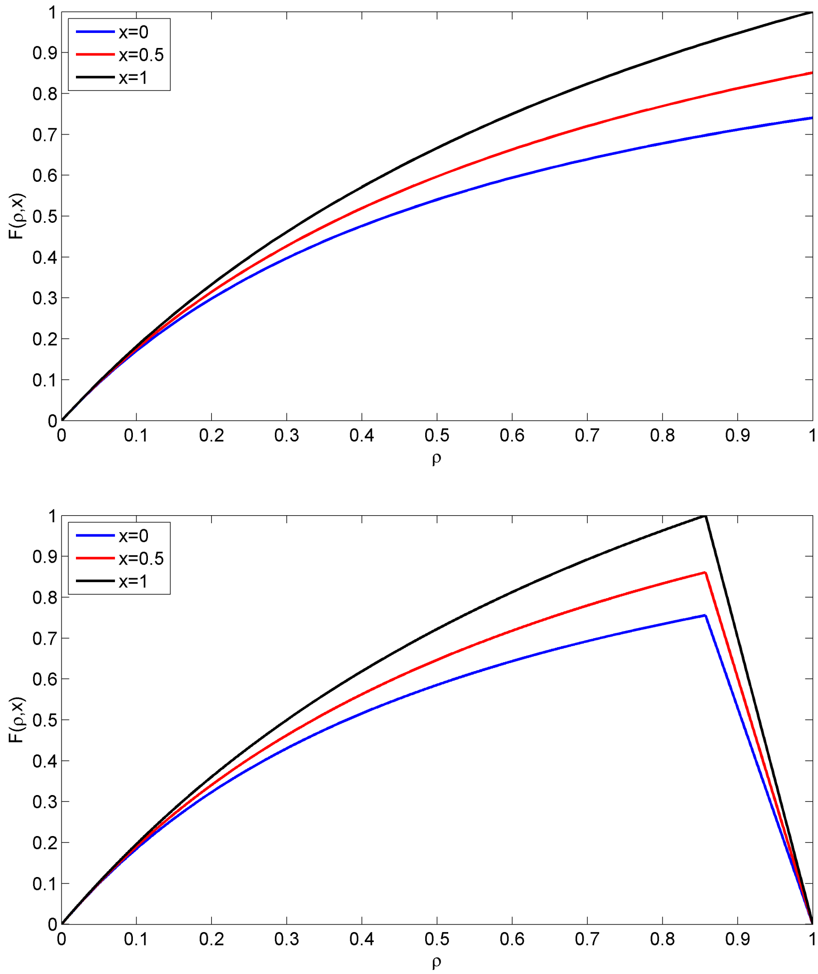

Figure 9: The discontinuous flux function (left) and a smoothed out version with $\rho^* = \frac{6}{7}$ (right).

total, for our choice of parameters, the CPU time consumed for solving the PDE-model is approximately 85 seconds for $\rho^* = \frac{6}{7}$, i.e. $\Delta t = 1.4287e - 004$ on an intel core duo 2.50GHz. That is an enormous advantage compared to particle-oriented approaches as for instance the discrete event simulations.

Snapshots of the solution for $\rho^* = \frac{6}{7}$ are shown in Figure 10 for $\lambda \approx \lambda_c$ and Figure 11 for $\lambda << \nu$, respectively. The results reflect the scenarios steady state, shutdown, and restarting of the last machine in accordance with the first three steps mentioned in Section 2, (Figure 3). Initially, we start with an empty system. We observe a ramp-up ending in a space-dependent steady state, (first picture in Figure 10 and Figure 11). Except for numerical inaccuracy, the steady state solution matches with Figure 2(a) and equation (12). Then, the last machine is shut down and parts are blocked. A WIP wave is moving backwards along the production line resulting in a steady state at maximum buffer level (second picture in Figure 10 and Figure 11) and stopped production. The system is restarted by opening the last machine. Parts may leave the system again and forward as well as backward moving waves are eating up the accumulated WIP. The associated Riemann problem $M = \rho_l > \rho_r$ leads to a wave traveling with high speed. Finally, the system returns into the steady state solution again (third picture in Figure 10 and Figure 11).

6 Conclusions

We have developed a continuum model of a production flow line with finite buffers as a transport equation for the WIP density. The model extends the quasi-static approximation of production lines based on using steady state clearing functions as the flux models of conservation laws [3]. Following Gershwin [22] and Gossens [23] we assumed a clearing function that, for the same WIP, has a higher flux at the beginning of the production line than at the end, corresponding to the higher probability of blocking away from the end of the production line. In addition, the flux function is discontinuous since, as the WIP takes on the value of the buffer limit, the upstream machine will have to shut down since it cannot deliver its product to the next buffer.

The resulting PDE model has been used to study the breakdown of the whole production line following a failure of the last machine, and the subsequent recovery of the production line after the last machine has been repaired. The study of the associated Riemann problem for the conservation law reveals the shutdown of the factory as a regular shock wave, traveling with the speed associated with the time needed to fill up the whole factory to the maximum WIP level. The Riemann problem for the re-opening of the production line depends crucially on the inflow: For a production line that is run significantly below capacity, a shock wave is generated at the beginning of the factory that corresponds to a transition from high WIP level (the blocked states) to the steady state of the WIP level associated with the much lower input. In addition, there is an outflow corresponding to the gradual removal of WIP from the end of the production line leading to a speed up of the shock wave as it moves forward. For an inflow corresponding to the maximally possible capacity of the production line the shock wave from the end disappears and the steady state is reached only through the much slower draining process from the end of the production line. Numerical simulations based on a smoothing out of the discontinuous flux function using a Lax-Friedrich scheme are performed.

There are a at least two interesting open problems associated with our model.

- Given a PDE model, we can solve the associated production planing problem. I.e. we can study the question, given a state of the system determined by a WIP distribution and given a desired output $d(t)$ over a time interval T, what is the influx that minimizes the mean square error of the outflux over T and the demand. This problem has been solved for the PDE model for unbounded buffers [30] but remains to be studied for the flow line with finite buffer. In particular for demand that temporarily exceeds the steady state flux values, the problem has become significantly more difficult, since the influx has to avoid creating blocked buffers.

- While there are first principle models for the derivation of the PDE model from a queuing network with unlimited buffers [2, 16], there exists no such theory for finite buffers. The most interesting regime in particular is the draining of a completely full production line. The resulting elementary processes are the generation of synchronous

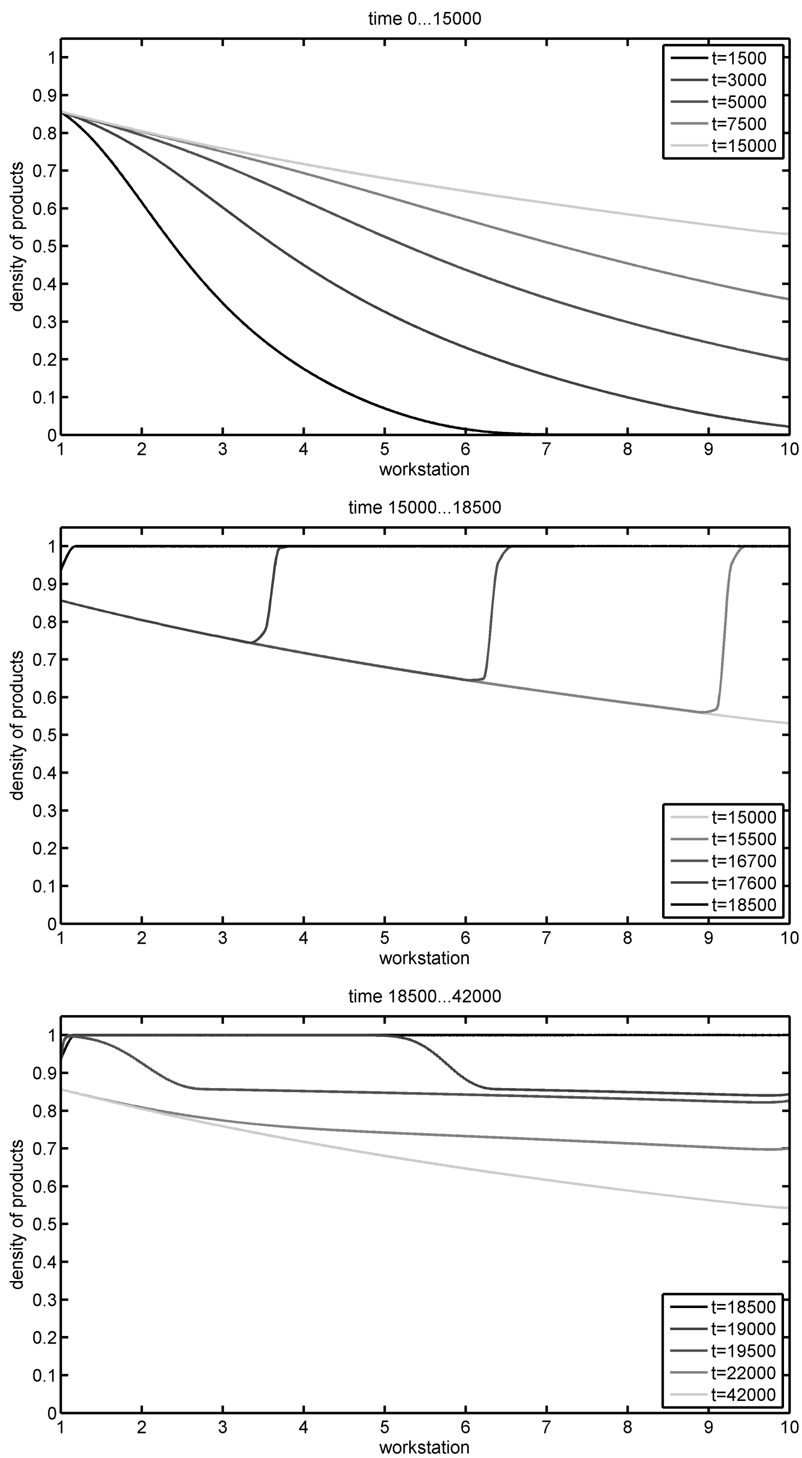

Figure 10: Observations for $\rho^* = \frac{6}{7}$ and $\lambda \approx \lambda_c$: 1) Ramp-up and steady state solution (top figure), 2) breakdown of the last machine (middle figure), and 3)+4) restarting production again and final equilibrium (bottom figure).

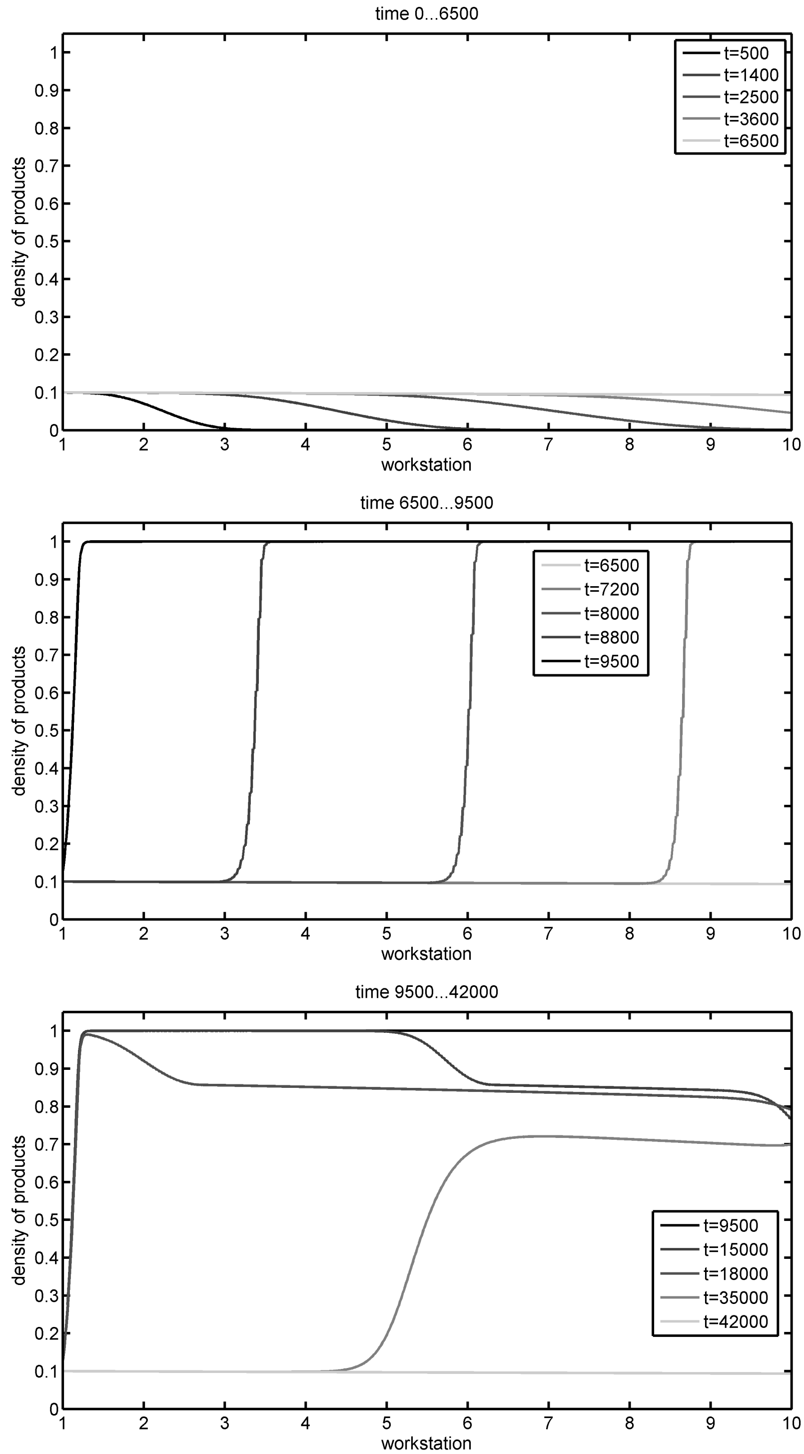

Figure 11: Observations for $\rho^* = \frac{6}{7}$ and $\lambda << \nu$: 1) Ramp-up and steady state solution (top figure), 2) breakdown of the last machine (middle figure), and 3)+4) restarting production again and final equilibrium (bottom figure).

avalanches along the production line: The newly active last machine will generate a synchronous motion of all machines. They drop their finished product into the single free space of the next downstream buffer and start a new product. When a particular machine i can start its next product depends on whether the buffers for $n > i$ are empty which depends in turn on the stochastic distribution of the cycle times. As a result, WIP moves along the production line in partially synchronized blocks. This is very close to models of the totally asymmetric exclusion process (TASEP) that has been studied for lattice gases [29, 35]. Here a particle enters a one-dimensional lattice from the left with a rate α and leaves it on the right with a rate β. In the interior, a particle can jump to a neighboring site with a constant probability provided that the site is empty. Spatially inhomogeneous steady states similar to the steady states of our WIP distributions have been derived analytically for large inflows and phase transitions as a function of the in- and outflow have been found. The challenge is to relate this model to a model that has time dependent α and β which happens when the decaying WIP at the end of the factory leads to a decaying outflux and the reduced blocking at the beginning of the line leads to a increased influx.

- Our model of the draining of the completely full production line shows an interplay between two fast time scales both of which are not modeled directly and are implicitly set by the numerical resolutions of the PDE simulations: Any adiabatic model based on mass conservation and a state equation for the dependence of the flux on the density is based on a closure assumption that any perturbation of the system out of the equilibrium instantaneously relaxes to the equilibrium relationship given by the state equation. This is in particular the case for the situation of the re-starting of production with completely full buffers. In addition, when the last machine restarts, there is the information wave traveling upstream. That wave in reality is moving with a close to infinite speed and in our model moves with the speed $\frac{1}{\epsilon}$ given by the smoothing of the clearing function over an interval of ϵ. A model based on a higher order closure adding an evolution equation for the velocity [2] will model the relaxation of the velocity and give us a better control over the interaction of these two fast time scales.

References

[1] D. Armbruster, P. Degond, and C. Ringhofer, *A model for the dynamics of large queuing networks and supply chains*, SIAM J. Applied Mathematics, 66 (2006), pp. 896–920.

[2] D. Armbruster, D. Marthaler, and C. Ringhofer, *Kinetic and fluid model hierarchies for supply chains*, Operations Research, 2 (2003), pp. 43–61.

[3] D. Armbruster, D. Marthaler, C. Ringhofer, K. Kempf, and T.-C. Jo, *A continuum model for a re-entrant factory*, Operations Research, 54 (2006), pp. 933–950.

[4] A. Aw, A. Klar, T. Materne, and M. Rascle, *Derivation of continuum traffic flow models from microscopic follow-the-leader models*, SIAM J. Appl. Math., 63 (2002), pp. 259–278.

[5] A. Aw and M. Rascle, *Resurrection of "second order" models of traffic flow*, SIAM J. Appl. Math., 60 (2000), pp. 916–938.

[6] M. K. Banda, M. Herty, and A. Klar, *Coupling conditions for gas networks governed by the isothermal Euler equations*, Netw. Heterog. Media, 1 (2006), pp. 295–314.

[7] C. Bardos, A. Y. le Roux, and J.-C. Nédélec, *First order quasilinear equations with boundary conditions*, Comm. Partial Differential Equations, 4 (1979), pp. 1017–1034.

[8] G. M. Coclite, M. Garavello, and B. Piccoli, *Traffic flow on a road network*, SIAM J. Math. Anal., 36 (2005), pp. 1862–1886.

[9] R. M. Colombo, P. Goatin, and F. S. Priuli, *Global well posedness of traffic flow models with phase transitions*, Nonlinear Anal., 66 (2007), pp. 2413–2426.

[10] R. M. Colombo, G. Guerra, M. Herty, and V. Schleper, *Optimal control in networks of pipes and canals*, SIAM J. Control Optim., 48 (2009), pp. 2032–2050.

[11] C. M. Dafermos, *Polygonal approximations of solutions of the initial value problem for a conservation law*, J. Math. Anal. Appl., 38 (1972), pp. 33–41.

[12] Y. Dallery and S. B. Gershwin, *Manufacturing flow line systems: A review of models and analytical results*, Oueueing Systems, 12 (1992), pp. 3–94.

[13] J. de Halleux, C. Prieur, J.-M. Coron, B. d'Andréa Novel, and G. Bastin, *Boundary feedback control in networks of open channels*, Automatica J. IFAC, 39 (2003), pp. 1365–1376.

[14] A. de Kok, *Computationally efficient approximations for balanced flowlines with finite intermediate buffers*, International Journal of Production Research, 28 (1990), pp. 410–419.

[15] P. Degond, S. Göttlich, M. Herty, and A. Klar, *A network model for supply chains with multiple policies*, Multiscale Model. Simul., 6 (2007), pp. 820–837.

[16] P. Degond and C. Ringhofer, *Stochastic dynamics of long supply chains with random breakdowns*, SIAM J. Applied Mathematics, 68 (2007), pp. 59–79.

[17] J.-P. Dias and M. Figueira, *On the Riemann problem for some discontinuous systems of conservation laws describing phase transitions*, Commun. Pure Appl. Anal., 3 (2004), pp. 53–58.

[18] ——, *On the approximation of the solutions of the Riemann problem for a discontinuous conservation law*, Bull. Braz. Math. Soc. (N.S.), 36 (2005), pp. 115–125.

[19] ——, *On the viscous Cauchy problem and the existence of shock profiles for a p-system with a discontinuous stress function*, Quart. Appl. Math., 63 (2005), pp. 335–341.

[20] J.-P. Dias, M. Figueira, and J.-F. Rodrigues, *Solutions to a scalar discontinuous conservation law in a limit case of phase transitions*, J. Math. Fluid Mech., 7 (2005), pp. 153–163.

[21] S. B. Gershwin, *An efficient decomposition method for the approximate evaluation of tandem queues with finite storage space and blocking*, Oper. Res., 35 (1987), pp. 291–305.

[22] S. B. Gershwin, *Manufacturing Systems Engineering*, Prentice Hall, Englewood Cliffs, NJ, 1994.

[23] P. Goossens, *Modeling of manufracturing systems with finite buffer sizes using pdes*, Masters Thesis, TU Eindhoven, Department of Mechanical Engineering, SE 420523, (2007).

[24] S. Göttlich, M. Herty, and A. Klar, *Network models for supply chains*, Commun. Math. Sci., 3 (2005), pp. 545–559.

[25] S. Göttlich, M. Herty, and C. Ringhofer, *Optimization of order policies in supply networks*, European J. Oper. Res., 202 (2010), pp. 456–465.

[26] M. Herty and A. Klar, *Simplified dynamics and optimization of large scale traffic networks*, Math. Models Methods Appl. Sci., 14 (2004), pp. 579–601.

[27] M. Herty and M. Rascle, *Coupling conditions for a class of second-order models for traffic flow*, SIAM J. Math. Anal., 38 (2006), pp. 595–616.

[28] H. Holden and N. H. Risebro, *A mathematical model of traffic flow on a network of unidirectional roads*, SIAM J. Math. Anal., 26 (1995), pp. 999–1017.

[29] A. Kolomeisky, G. Schütz, E. Kolomeisky, and J. Straley, *Phase diagram of one-dimensional driven lattice gases with open boundaries*, J.Phys. A: Math. Gen., 31 (1998), pp. 6911–6919.

[30] M. La Marca, D. Armbruster, M. Herty, and C. Ringhofer, *Control of continuum models of production systems*, IEEE Transactions on automatic control, to appear (2010).

[31] J. P. Lebacque, X. Louis, S. Mammar, B. Schnetzler, and H. Haj-Salem, *Modélisation du trafic autoroutier au second ordre*, C. R. Math. Acad. Sci. Paris, 346 (2008), pp. 1203–1206.

[32] M. J. Lighthill and G. B. Whitham, *On kinematic waves. II. A theory of traffic flow on long crowded roads*, Proc. Roy. Soc. London. Ser. A., 229 (1955), pp. 317–345.

[33] J. Little, *A proof for the queueing formula $l = \lambda w$*, Operations Research, 9 (1961), pp. 383–387.

[34] D. Perdaen, D. Armbruster, K. Kempf, and E. Lefeber, *Controlling a re- entrant manufacturing line via the push-pull point*, International Journal of Production Research, 46 (2008), pp. 4521– 4536.

[35] G. Schütz and E. Domany, *Phase transitions in an exactly soluble one-dimensional exclusion process*, Journal of Statistical Physics, 72 (1993), pp. 277–296.

[36] D. A. van Beek, K. L. Man, M. A. Reniers, J. E. Rooda, and R. R. H. Schiffelers, *Syntax and consistent equation semantics of hybrid chi*, J. Log. Algebr. Program., 68 (2006), pp. 129–210.

Acknowledgements

This work was financially supported by the DAAD research grants no. D/08/11076, 50727872, 50021880 and the DFG project HE5386/6-1 and HE5386/8-1. D.A. was supported by a grant from the Stiftung Volkswagenwerk under the program on Complex Networks and by NSF grant DMS-0604986. We want to thank Christian Ringhofer for fruitful discussions and Erjen Lefeber and Puck Gossens for movies, figures and explanation of their discrete event simulations.